Accurate Measurements of the Acoustical Physical Constants of $LiNbO_3$ and $LiTaO_3$ Single Crystals

Jun-ichi Kushibiki, *Member, IEEE*, Izumi Takanaga, Mototaka Arakawa, and Toshio Sannomiya

***Abstract*—The acoustical physical constants (elastic constant, piezoelectric constant, dielectric constant, and density) of commercial surface acoustic wave (SAW)-grade $LiNbO_3$ and $LiTaO_3$ single crystals were determined by measuring the bulk acoustic wave velocities, dielectric constants, and densities of many plate specimens prepared from the ingots. The maximum probable error in each constant was examined by considering the dependence of each constant on the measured acoustic velocities. By comparing the measured values of longitudinal velocities that were not used to determine the constants with the calculated values using the previously mentioned constants, we found that the differences between the measured and calculated values were 1 m/s or less for both $LiNbO_3$ and $LiTaO_3$ crystals. These results suggest that the acoustical physical constants determined in this paper can give the values of bulk acoustic wave velocities with four significant digits.**

I. Introduction

$LiNbO_3$ and $LiTaO_3$ single crystals are widely used as substrates for bulk wave and SAW devices. Therefore, it is important to know accurately the acoustical physical constants (elastic constant c^E, piezoelectric constant e, dielectric constant ε^S, and density ρ) of these crystals for analyzing the propagation characteristics of acoustic waves and for designing devices. Although the acoustical physical constants have been reported in many papers [1]–[12], the problem is that the constants depend on the chemical compositions and crystal growth conditions, largely differing from those in the initial stage of the research and development and resulting in different bulk and SAW velocities. Recently, the acoustical physical constants for commercial wafers with a congruent chemical composition have been determined using data of SAW velocities [10], [12]. However, because the dielectric constants and densities reported elsewhere were used for the determination, some uncertain errors in the determined constants may be involved.

In this paper, we determine all independent components of the acoustical physical constants of $LiNbO_3$ and $LiTaO_3$ single crystals with high accuracy by preparing many plate specimens from ingots of commercially available SAW-grade $LiNbO_3$ and $LiTaO_3$ single crystals, suitable for precise determination, and by measuring their bulk acoustic wave velocities, dielectric constants, and densities.

Manuscript received February 23, 1999; accepted April 20, 1999. This work was supported in part by a Research Grant-in-Aid from the Japan Ministry of Education, Science and Culture.

The authors are with Department of Electrical Engineering, Tohoku University, Sendai 980-8579, Japan (e-mail: kushi@ecei.tohoku.ac.jp).

TABLE I
$LiNbO_3$ and $LiTaO_3$ Single Crystals for Determining the Acoustical Physical Constants.

	$LiNbO_3$	$LiTaO_3$
Pulling axis	Z	Y
Diameter (mm)	100	100
Length (mm)	99	85

II. Preparation of Specimens

To determine the acoustical physical constants, we prepared the ingots of SAW-grade $LiNbO_3$ and $LiTaO_3$ single crystals grown by the Czochralski method (Yamaju Ceramics Co., Ltd., Seto, Japan). The crystal pulling axis, diameter, and length of each ingot are shown in Table I. To investigate the homogeneity of the elastic properties of ingots, three substrates were cut perpendicular to the crystal pulling axis from the top, middle, and bottom portions of each ingot as shown in Fig. 1. The velocities of leaky SAWs (LSAWs) that propagate on the water-loaded specimen surfaces, longitudinal acoustic wave velocities, densities, lattice constants, and Curie temperatures were then measured. The results are detailed in the literature [13]. For both crystals, we estimated that the distributions in acoustic properties of LSAW and longitudinal acoustic wave velocities are about 1 m/s in the pulling axis direction and that the corresponding chemical composition ratio in the ingot varied about 0.02 Li_2O-mol%.

Eighteen $LiNbO_3$ and 16 $LiTaO_3$ crystal substrate specimens were cut from each ingot. Each specimen was about 4 mm thick, and both sides were optically polished. To determine the propagation direction of ultrasonic waves accurately so that the inclination between the crystalline plane and the specimen surface could be checked using X-ray analysis, all specimens were selected from the crystalline planes specified in the American Society for Testing and Materials (ASTM) cards ($LiNbO_3$: No. 20-631; $LiTaO_3$: No. 29-836). Rotated Y-cut specimens (rotating a Y-cut specimen about the X axis) were cut from the upper-half block of each ingot. Three principal X-, Y-,

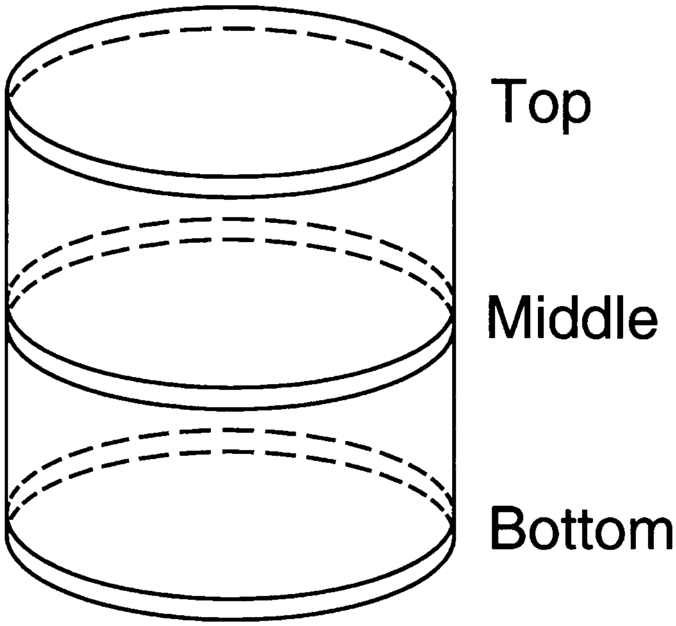

Fig. 1. Specimen preparation.

and Z-cut specimens, rotated X-cut specimens (rotating an X-cut specimen about the Y axis), and Z-axis cylinder specimens (rotating an X-cut specimen about the Z axis) were then cut from the intermediate substrate and lower-half block. The acoustic velocities are measured at the center of each specimen, and the measurement positions are located within one-half the ingot range about the intermediate substrate in the pulling axis direction. Therefore, the variation of the acoustic velocities in the pulling axis direction used to determine the acoustical physical constants is estimated to be at most 0.5 m/s ($\pm$0.25 m/s for the average). Because this variation is about the same magnitude as the measurement accuracy of the acoustic velocity ($\pm$0.30 m/s), the ingots used in this paper can be considered to be almost homogeneous within the velocity measurement accuracy.

The inclination angles between the crystalline planes and the specimen surfaces were measured on all the specimens by X-ray analysis and were found to be 0.12° maximum and less than 0.10° for most specimens. These inclinations can be compensated through numerical calculations.

III. Procedure of Determination

$LiNbO_3$ and $LiTaO_3$ single crystals belong to class 3m of trigonal system, in which there is a total of 13 independent acoustical physical constants. Taking the strain S and the electric field E as the independent variables, there are six elastic stiffness constants [c_{11}^E $(= c_{12}^E + 2c_{66}^E)$, c_{12}^E, c_{13}^E, c_{14}^E, c_{33}^E, and c_{44}^E], four piezoelectric stress constants (e_{15}, e_{22}, e_{31}, and e_{33}), and two dielectric constants at constant strain (ε_{11}^S and ε_{33}^S) and density (ρ). In this paper, the acoustical physical constants are determined using bulk waves for which the relationship between acoustic velocities and acoustical physical constants is relatively simple and, in general, expressed in the following equation:

$$V = \sqrt{\frac{c^E + \frac{e^2}{\varepsilon^S}}{\rho}}. \tag{1}$$

It can be seen from (1) that it is necessary to measure not only acoustic velocities but also dielectric constants and density to determine all of the independent constants. As for the dielectric constant, ε_{11}^S can be measured using an X-cut or Y-cut specimen, and ε_{33}^S can be measured using a Z-cut specimen.

To determine each constant with high accuracy, it is necessary not only to measure acoustic velocities, dielectric constants, and density with high accuracy but also to select appropriately the propagation directions and the bulk wave modes. To find the appropriate direction and mode of the bulk wave, the equations between the acoustic velocities and the constants to be determined are as simple as possible, and the constants to be determined depend heavily on the acoustic velocities.

For bulk acoustic waves propagating along the X, Y, and Z axes, the X-axis longitudinal velocity $V_{X\ell}$, Z-axis shear velocity V_{Zs}, and Y-axis shear velocity with X-axis polarized particle displacement V_{YsX}, are related simply to the elastic constants in the following equations:

$$\rho V_{X\ell}^2 = c_{11}^E, \tag{2}$$

$$\rho V_{Zs}^2 = c_{44}^E, \text{ and} \tag{3}$$

$$\rho V_{YsX}^2 = c_{66}^E = (c_{11}^E - c_{12}^E)/2, \text{ respectively.} \tag{4}$$

The constants c_{11}^E, c_{44}^E, and c_{66}^E can thus be determined independently from these three acoustic velocities and the density. The rotated Y-axis shear velocity with X-axis polarized particle displacement, V_{rYsX}, having the rotation angle θ, about the X axis from the Y axis to the Z axis, is represented as

$$\rho V_{rYsX}^2 = c_{14}^E \sin 2\theta + c_{44}^E \sin^2\theta + c_{66}^E \cos^2\theta. \tag{5}$$

Using the (5), c_{14}^E can be determined with the measured velocity of V_{rYsX} and the previously determined c_{44}^E and c_{66}^E.

Furthermore, the following equations relate the X-axis shear velocity V_{Xs} and Y-axis longitudinal velocity $V_{Y\ell}$ to the acoustical physical constants:

$$\begin{vmatrix} c_{66}^E - \rho V_{Xs}^2 & c_{14}^E & -e_{22} \\ c_{14}^E & c_{44}^E - \rho V_{Xs}^2 & e_{15} \\ -e_{22} & e_{15} & -\varepsilon_{11}^S \end{vmatrix} = 0 \tag{6}$$

and

$$\begin{vmatrix} c_{11}^E - \rho V_{Y\ell}^2 & -c_{14}^E & e_{22} \\ -c_{14}^E & c_{44}^E - \rho V_{Y\ell}^2 & e_{15} \\ e_{22} & e_{15} & -\varepsilon_{11}^S \end{vmatrix} = 0. \tag{7}$$

Because the four elastic constants in these two expressions were determined previously, e_{15} and e_{22} can be determined

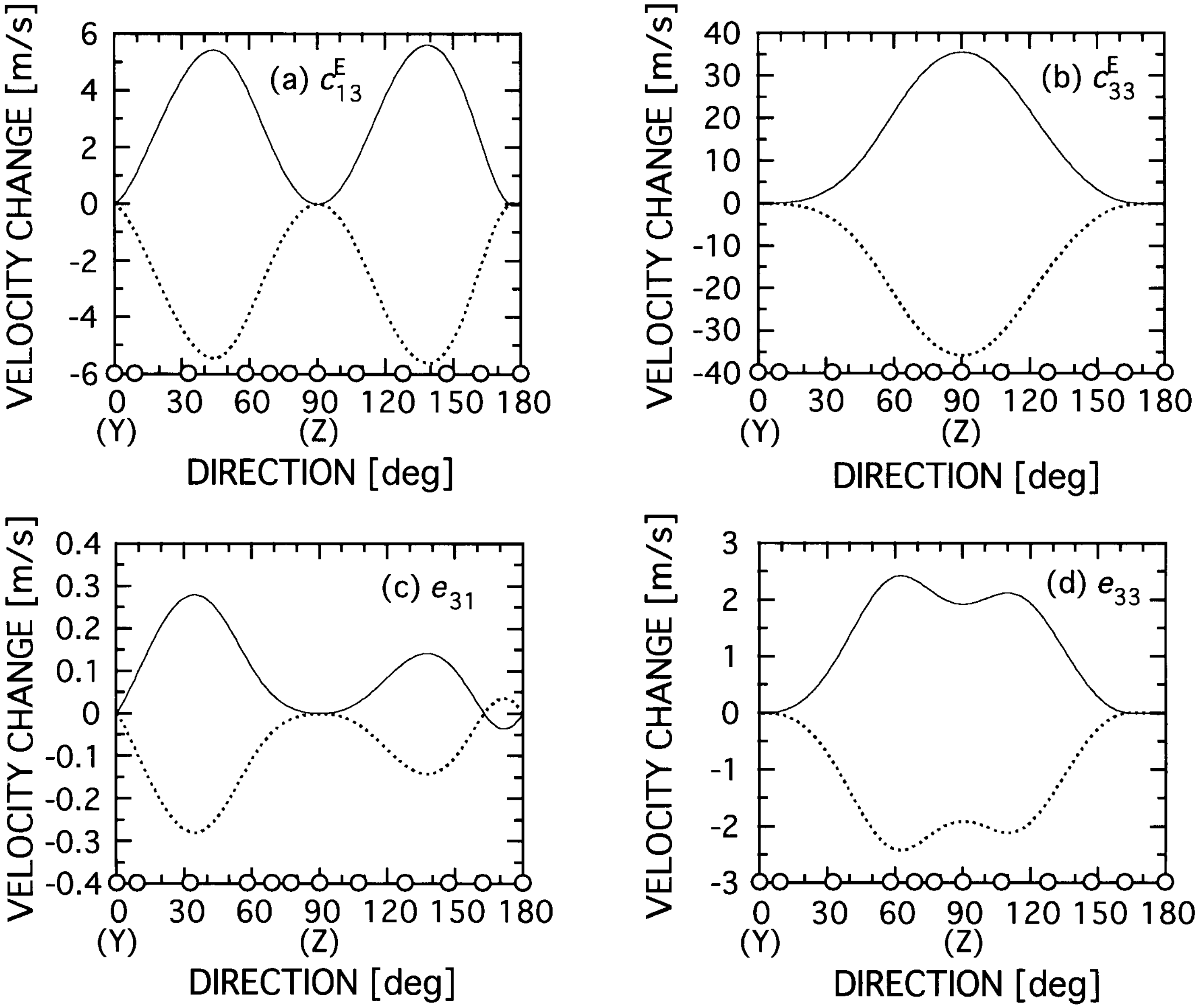

Fig. 2. Longitudinal velocity changes influenced by 1% increase and decrease of the published acoustical physical constants of $LiNbO_3$ [1]. Solid line = +1%, dotted line = −1%, o = angles of the crystalline planes on ASTM card.

from these two velocities. In this case, for two X-axis shear waves, the higher shear wave velocity with the larger electromechanical coupling factor is used.

Lastly, the remaining constants (c^E_{13}, c^E_{33}, e_{31}, and e_{33}) are determined using the longitudinal velocities for four rotated Y-cut specimens, including a Z-cut specimen. The rotated Y-axis longitudinal velocities $V_{rY\ell}$ are related to the acoustical physical constants in the following equation:

$$\begin{vmatrix} c^{E\prime}_{11} - \rho V^2_{rY\ell} & c^{E\prime}_{16} & e'_{11} \\ c^{E\prime}_{16} & c^{E\prime}_{66} - \rho V^2_{rY\ell} & e'_{16} \\ e'_{11} & e'_{16} & -\varepsilon^{S\prime}_{11} \end{vmatrix} = 0. \tag{8}$$

The primed constants indicate that the constants have been subjected to coordinate transformation for the desired propagation direction. The constants $c^{E\prime}_{11}$, $c^{E\prime}_{16}$, and $c^{E\prime}_{66}$ are all functions of the five elastic constants except for c^E_{12} and the rotation angle θ for the rotated Y-cut specimen; e'_{11} and e'_{16} are functions of the four piezoelectric constants and the rotation angle θ; and $\varepsilon^{S\prime}_{11}$ is a function of the two dielectric constants and the rotation angle θ. To determine c^E_{13}, c^E_{33}, e_{31}, and e_{33} with high accuracy, it is necessary to select a proper propagation direction for which these constants have a large dependence on measured velocities. Therefore, we examined the longitudinal velocity changes while each constant (c^E_{13}, c^E_{33}, e_{31}, and e_{33}) varies within the range of ±1% using the value in the literature [1]. Calculations for $LiNbO_3$ are shown in Fig. 2. For each constant, the crystalline plane that shows the largest velocity change of the crystalline planes specified in the ASTM card (i.e., (306) plane (147.24° Y-cut) for c^E_{13}, (006) plane (Z-cut) for c^E_{33}, (012) plane (32.76° Y-cut) for e_{31}, and (02$\underline{10}$) plane (58.13° Y-cut) for e_{33}) is selected as the specimen. Specimens for $LiTaO_3$ are selected in the same manner.

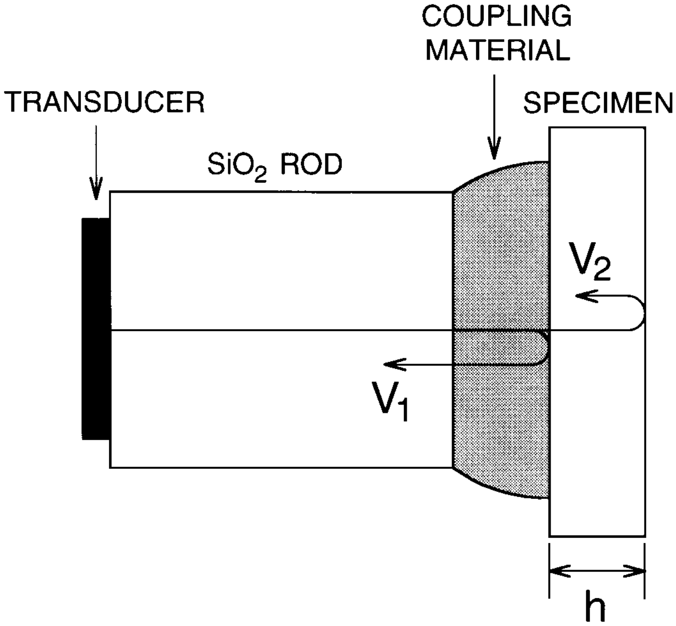

Fig. 3. Experimental arrangement of bulk wave ultrasonic velocity measurements by the pulse interference method.

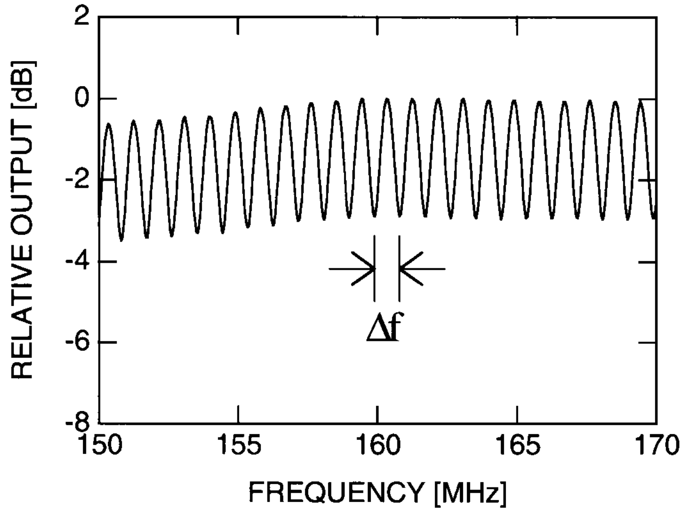

Fig. 4. Frequency response of interference output for a Z-cut $LiNbO_3$ specimen in longitudinal wave velocity measurement by the pulse interference method. The specimen thickness is 4029.5 μm.

IV. Measurement Methods and Results

Velocities are mainly measured by the bulk ultrasonic pulse interference method using radio frequency (RF) tone burst signals [14], [15]. Fig. 3 shows the experimental arrangement for velocity measurement. Two plane wave ultrasonic devices for velocity measurements were prepared with a ZnO piezoelectric film transducer for longitudinal waves and an X-cut $LiNbO_3$ transducer for shear waves on cylindrical buffer rods of synthetic silica (SiO_2) glass. Coupling materials are pure water for longitudinal waves and a thin layer of bonding material salol (phenyl salicylate) for shear waves. Signals converted to acoustic waves propagate through the rod, couplant, and specimen as the waves are reflected and transmitted at each boundary and are reflected perfectly at the back surface of the specimen. When signals reflected from the front surface of the specimen, V_1, and from the back surface, V_2, are superposed in the time domain by the double-pulse method and the frequency is swept, the interference waveform shown in Fig. 4 is obtained. The velocity, V, is determined from the frequency interval in the interference waveform, Δf, and the thickness of the specimen, h, using the following equation:

$$V = 2\Delta f h. \tag{9}$$

The specimen thickness is measured by a digital length gauging system with an accuracy of ± 0.1 μm. Here, the velocity measurement accuracy mainly depends on the thickness measurement accuracy (five significant figures). In shear velocity measurements, the influence of the phase change in the bonding layer on the acoustic velocity is compensated.

Using the ultrasonic pulse interference method, shear velocity can be accurately measured only when the particle displacement is independent. The shear velocity when the particle displacement is not independent (i.e., X-axis shear velocity) is measured using a thickness mode resonator [16]. The acoustic velocity is obtained from the antiresonance frequency, f_a, specimen thickness, h, and order of overtone, n, using the following equation:

$$V = 2 f_a h / n. \tag{10}$$

The dielectric constant is obtained by measuring the capacitance of a plate with full electrodes. If the measurement frequency is set sufficiently lower than the lowest resonance frequency, the dielectric constant at constant stress, ε^T, can be measured with high accuracy. The dielectric constant at constant strain, ε^S, is then calculated using the following equation [16]:

$$\varepsilon^S_{ij} = \varepsilon^T_{ij} - e_{ip} s^E_{pq} e_{jq} \tag{11}$$

where $s^E$is the elastic compliance constant and is related by $s^E = (c^E)^{-1}$.

Density is measured based on the Archimedes method [17].

The acoustic velocities measured for the respective crystals are shown in Table II and Table III. The velocity was measured by the pulse interference method at around 150 MHz for longitudinal waves and 100 MHz for shear waves. The frequency range for measuring shear velocity by the resonance method is 3 to 13 MHz. The measured dielectric constants at constant stress and density are shown in Table IV. The dielectric constants were measured at around 10 kHz, and all measurements were performed at around 23.0°C.

V. Determination and Errors

The acoustical physical constants of $LiNbO_3$ and $LiTaO_3$ single crystals as determined are shown in Table V

TABLE II
MEASURED VELOCITIES OF $LiNbO_3$ SPECIMENS USED FOR DETERMINATION.

Mode	Method	Specimen		Velocity (m/s)
Longitudinal wave	Pulse interference method	(300)	Y	6806.55 ± 0.26
		(012)	32.76° Y	7338.65 ± 0.31
		$(02\underline{10})$	58.13° Y	7314.62 ± 0.31
		(006)	Z	7328.20 ± 0.32
		(306)	147.24° Y	6855.49 ± 0.29
		(110)	X	6544.53 ± 0.30
Shear wave	Pulse interference method	(300)	Y	3940.49 ± 0.21
		(104)	127.85° Y	3499.94 ± 0.21
		(006)	Z	3590.41 ± 0.23
	Resonance method	(110)	X	4750.67 ± 0.59

TABLE III
MEASURED VELOCITIES OF $LiTaO_3$ SPECIMENS USED FOR DETERMINATION.

Mode	Method	Specimen		Velocity (m/s)
Longitudinal wave	Pulse interference method	(300)	Y	5746.11 ± 0.25
		(012)	32.98° Y	6332.93 ± 0.35
		(006)	Z	6174.94 ± 0.35
		$(10\underline{10})$	107.13° Y	6174.73 ± 0.28
		(306)	147.02° Y	5752.84 ± 0.26
		(110)	X	5589.17 ± 0.25
Shear wave	Pulse interference method	(300)	Y	3536.56 ± 0.18
		$(02\underline{10})$	58.35° Y	3377.72 ± 0.17
		(006)	Z	3573.30 ± 0.29
	Resonance method	(110)	X	4214.48 ± 0.62

TABLE IV
MEASURED DIELECTRIC CONSTANTS AND DENSITIES FOR $LiNbO_3$ AND $LiTaO_3$ SINGLE CRYSTALS.

		$LiNbO_3$	$LiTaO_3$
Dielectric constant	$\varepsilon_{11}^T/\varepsilon_0$	83.3 ± 0.8	53.0 ± 0.5
	$\varepsilon_{33}^T/\varepsilon_0$	28.5 ± 0.3	43.4 ± 0.4
Density (kg/m^3)	ρ	4642.8 ± 0.2	7460.4 ± 0.4

and Table VI together with two representative well-known values found in the literature [1], [10]. When measurement errors were ± 0.3 m/s for acoustic velocity, $\pm 1\%$ for dielectric constant, and $\pm 0.005\%$ for density, the maximum error of each constant was estimated using the following method.

If the independent variables of acoustical physical constants are denoted by x_i ($i = 1$ to 13) and the measured acoustic velocities, dielectric constants, and density by y_j ($j = 1$ to 13), each measurement value can be expressed as follows:

$$y_j = f_j(x_i). \tag{12}$$

If the measurement error Δy_j is contained in the measured value and the error in the constant to be determined is denoted by Δx_i, (12) can be expressed as follows:

$$y_j + \Delta y_j = f_j(x_i + \Delta x_i). \tag{13}$$

When (13) is expanded around variables x_i by the Taylor theorem and the second and higher order terms are ignored because of their minor errors, the following equation for errors can be obtained:

$$\Delta y_j = \frac{\partial f_j}{\partial x_1}\Delta x_1 + \cdots + \frac{\partial f_j}{\partial x_{13}}\Delta x_{13}. \tag{14}$$

Solving this equation as simultaneous equations of $j = 1$ to 13, the following equation can be obtained:

$$\Delta x_i = a_{ij}\Delta y_j. \tag{15}$$

Therefore, the maximum error $|\Delta x_i|_{\max}$ that may occur in variable x_i can be expressed as follows:

$$|\Delta x_i|_{\max} = |a_{ij}|\,|\Delta y_j|\,. \tag{16}$$

The errors of c_{11}^E and c_{44}^E, which can be determined from a single velocity, are very small, but the errors of c_{13}^E, c_{33}^E, e_{31}, and e_{33}, which are determined using multiple velocities, are relatively large. This is because the errors of c_{11}^E and c_{44}^E can be obtained in (16) by summing two terms representing a single velocity and density, but the errors of c_{13}^E, c_{33}^E, e_{31}, and e_{33} are obtained by summing 13 terms. However, the probability of the maximum error occurring in those constants determined from multiple velocities is very small.

We compared the measured values of longitudinal velocity that were not used to determine the constants with

TABLE V
Measured and Published Acoustical Physical Constants of $LiNbO_3$ Single Crystal.

		Measured	Warner *et al.* [1]	Kovacs *et al.* [10]
Elastic constant ($\times 10^{11}$ N/m^2)	c_{11}^E	1.9886 ±0.0003	2.03	1.9839 ±0.0089
	c_{12}^E	0.5467 ±0.0004	0.53	0.5472 ±0.0097
	c_{13}^E	0.6799 ±0.0055	0.75	0.6513 ±0.0193
	c_{14}^E	0.0783 ±0.0002	0.09	0.0788 ±0.0004
	c_{33}^E	2.3418 ±0.0075	2.45	2.2790 ±0.0324
	c_{44}^E	0.5985 ±0.0001	0.60	0.5965 ±0.0008
	c_{66}^E	0.7209 ±0.0002	0.75	0.7184
Piezoelectric constant (C/m^2)	e_{15}	3.655 ±0.022	3.7	3.69 ±0.06
	e_{22}	2.407 ±0.015	2.5	2.42 ±0.04
	e_{31}	0.328 ±0.032	0.2	0.30 ±0.08
	e_{33}	1.894 ±0.054	1.3	1.77 ±0.12
Dielectric constant	$\varepsilon_{11}^S/\varepsilon_0$	44.9 ±0.4	44	45.6 ±1.5
	$\varepsilon_{33}^S/\varepsilon_0$	26.7 ±0.3	29	26.3 ±1.6
Density (kg/m^3)	ρ	4642.8 ±0.2	4.7×10^3	4628

the calculated values using the constants determined previously. The results for $LiNbO_3$ and $LiTaO_3$ single crystals are shown in Table VII and Table VIII. For both crystals, the differences between the measured and calculated values were 1 m/s or less. These results indicate that the acoustical physical constants determined above yield bulk acoustic wave velocities with an accuracy of four significant digits.

VI. Discussion

The acoustical physical constants for $LiNbO_3$ and $LiTaO_3$ single crystals published so far in the literature [10] were mostly reliable, especially for SAW calculations because they were determined from SAW measurements for commercially available SAW wafers produced from congruent crystals [18]. We calculated the longitudinal velocities of all specimens used in the previously mentioned experiments using the constants in the literature [10] and compared the results with the measured values. The results for $LiNbO_3$ and $LiTaO_3$ are shown in Table IX and Table X. Remarkable differences in velocity were observed in almost all propagation directions. The maximum difference in velocity observed in $LiNbO_3$ was more than 100 m/s, and that in $LiTaO_3$ was more than 10 m/s.

TABLE VI
Measured and Published Acoustical Physical Constants of $LiTaO_3$ Single Crystal.

		Measured	Warner *et al.* [1]	Kovacs *et al.* [10]
Elastic constant ($\times 10^{11}$ N/m^2)	c_{11}^E	2.3305 ±0.0004	2.33	2.328 ±0.036
	c_{12}^E	0.4644 ±0.0006	0.47	0.465 ±0.046
	c_{13}^E	0.8346 ±0.0067	0.80	0.836 ±0.043
	c_{14}^E	−0.1075 ±0.0004	−0.11	−0.105 ±0.002
	c_{33}^E	2.7522 ±0.0114	2.75	2.759 ±0.050
	c_{44}^E	0.9526 ±0.0002	0.94	0.949 ±0.004
	c_{66}^E	0.9331 ±0.0002	0.93	0.932
Piezoelectric constant (C/m^2)	e_{15}	2.628 ±0.022	2.6	2.64 ±0.27
	e_{22}	1.831 ±0.015	1.6	1.86 ±0.10
	e_{31}	−0.145 ±0.067	0.0	−0.22 ±0.28
	e_{33}	1.849 ±0.118	1.9	1.71 ±0.55
Dielectric constant	$\varepsilon_{11}^S/\varepsilon_0$	41.9 ±0.4	41	40.9 ±3.9
	$\varepsilon_{33}^S/\varepsilon_0$	41.8 ±0.4	43	42.5 ±2.6
Density (kg/m^3)	ρ	7460.4 ±0.4	7.45×10^3	7454

TABLE VII
Comparison of Longitudinal Wave Velocities Measured for other $LiNbO_3$ Crystalline Planes with those Calculated from the Determined Constants.

Specimen		Measured (m/s)	Calculated (m/s)	Difference (m/s)
(042)	9.14° Y	6998.21	6999.20	+0.99
(018)	68.77° Y	7305.47	7305.42	−0.05
$(01\underline{14})$	77.48° Y	7315.95	7316.01	+0.06
$(10\underline{10})$	107.27° Y	7298.94	7298.78	−0.16
(104)	127.85° Y	7158.99	7158.76	−0.23
(202)	162.17° Y	6656.29	6655.91	−0.38
(223)	15.57° X	6714.03	6713.61	−0.42
(113)	29.13° X	6970.74	6970.49	−0.25
(229)	39.89° X	7128.89	7128.17	−0.72
(116)	48.10° X	7206.55	7205.91	−0.64
$(11\underline{12})$	65.84° X	7286.28	7285.57	−0.71
(410)	100.89° X(Z)	6738.03	6738.77	+0.74

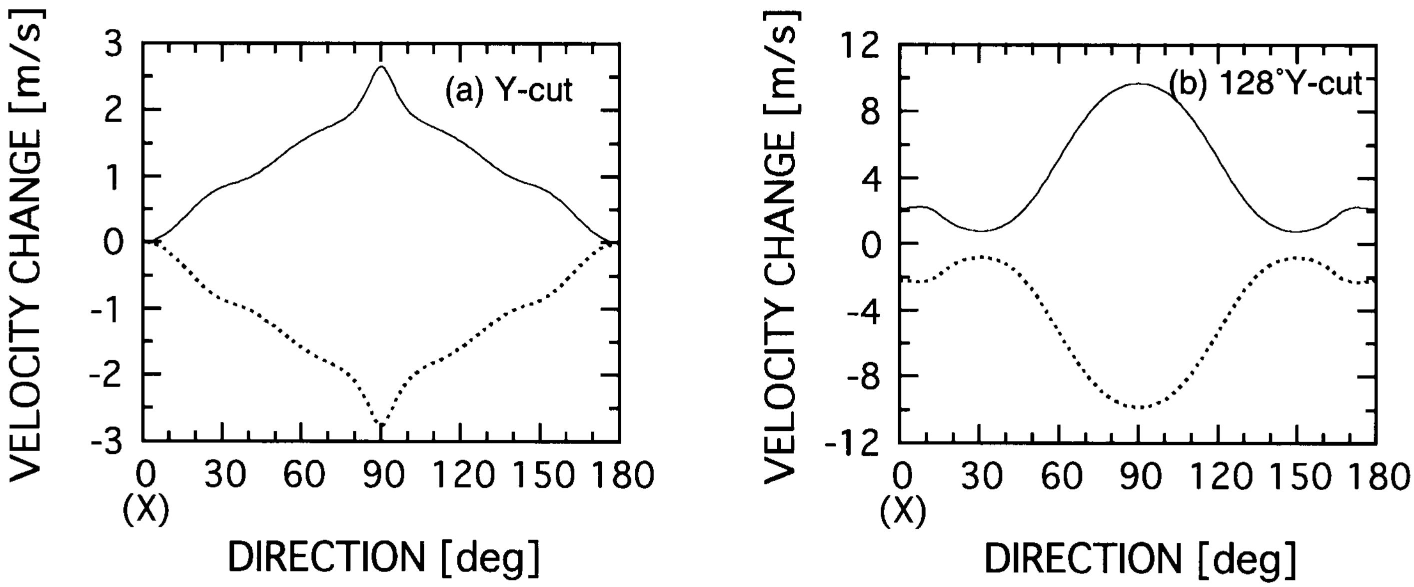

Fig. 5. SAW velocity changes influenced by a 1% increase and decrease of the published c_{33}^E of $LiNbO_3$ [1]. Solid line = +1%; dotted line = −1%.

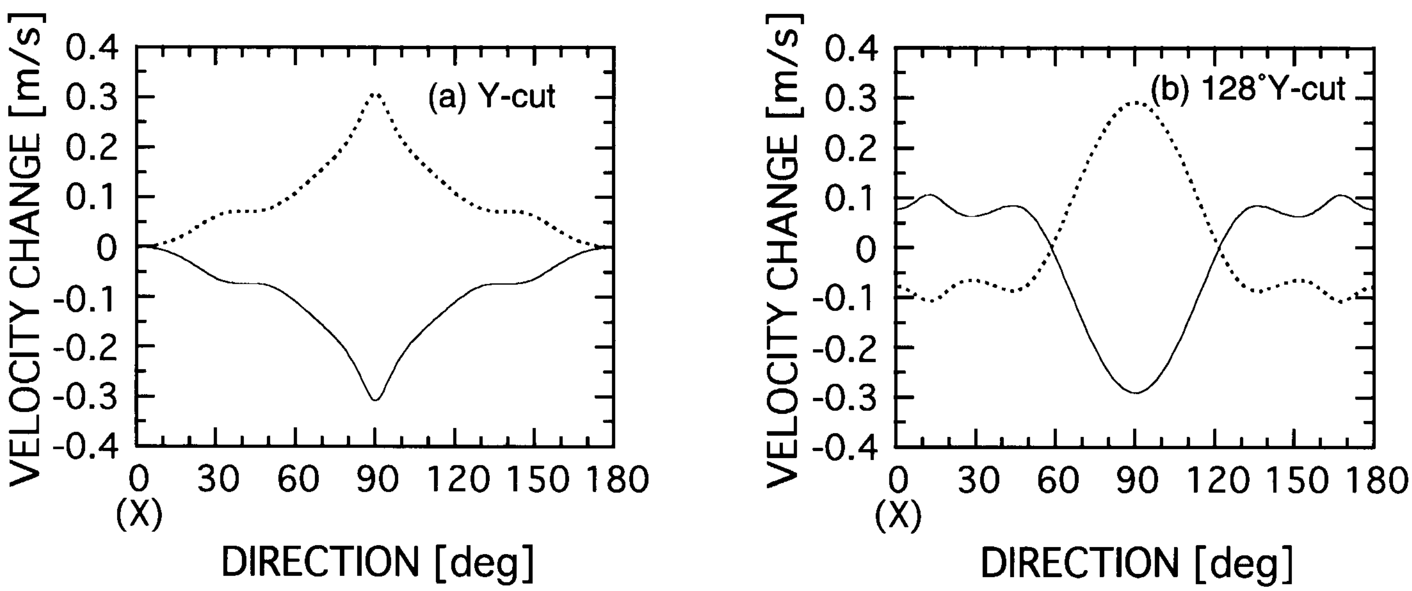

Fig. 6. SAW velocity changes influenced by a 1% increase and decrease of the published e_{33} of $LiNbO_3$ [1]. Solid line = +1%; dotted line = −1%.

The largest difference between the measured and calculated values was observed in the Z-axis longitudinal velocity for $LiNbO_3$, in which four acoustical physical constants, c_{33}^E, e_{33}, ε_{33}^S, and ρ, are involved. The literature [10] referred to the values for the dielectric constants at constant stress and density in other literature. The accuracies of c_{33}^E and e_{33} reported are questionable. Therefore, we investigated SAW velocity changes for the free and shorted surface conditions while varying c_{33}^E and e_{33} by ±1% on the Y-cut and 128° Y-cut $LiNbO_3$ substrates, which were used to determine the constants in the literature [10], in the same manner as in Section III and using the values in the literature [1]. The SAW velocity changes for the open surface condition with varying c_{33}^E and e_{33} are shown in Fig. 5 and 6. It can be seen that the dependences are small even in the direction of the largest dependence and are only one-quarter for c_{33}^E and one-tenth for e_{33} as compared with the dependences for the longitudinal velocities shown in Fig. 2. Therefore, we can say that the values of c_{33}^E and e_{33} from SAW velocities are determined less accurately than those from longitudinal velocities, resulting in a very large difference of 107 m/s for the Z-axis longitudinal velocity in $LiNbO_3$.

These discussions suggest that the accuracy of determining some constants in the literature [10] is poor because specimens and propagation directions with low de-

TABLE VIII
COMPARISON OF LONGITUDINAL WAVE VELOCITIES MEASURED FOR OTHER $LiTaO_3$ CRYSTALLINE PLANES WITH THOSE CALCULATED FROM THE DETERMINED CONSTANTS.

Specimen		Measured (m/s)	Calculated (m/s)	Difference (m/s)
(042)	9.21° Y	5965.66	5965.83	+0.17
$(02\underline{10})$	58.35° Y	6289.55	6289.83	+0.28
(018)	68.93° Y	6226.76	6226.93	+0.17
(104)	127.62° Y	6058.13	6058.32	+0.19
(202)	162.03° Y	5543.54	5543.19	−0.35
(113)	29.33° X	5995.42	5995.03	−0.39
(116)	48.34° X	6179.72	6179.03	−0.69
(119)	59.32° X	6204.09	6203.45	−0.64
$(11\underline{12})$	66.02° X	6201.17	6200.73	−0.44
(410)	100.89° X(Z)	5705.21	5704.91	−0.30

TABLE IX
COMPARISON OF LONGITUDINAL WAVE VELOCITIES MEASURED FOR $LiNbO_3$ SPECIMENS WITH THOSE CALCULATED USING KOVACS' CONSTANTS.

Specimen		Measured (m/s)	Calculated (m/s)	Difference (m/s)
(300)	Y	6806.55	6808.63	+2.08
(042)	9.14° Y	6998.21	6996.18	−2.03
(012)	32.76° Y	7338.65	7307.85	−30.80
$(02\underline{10})$	58.13° Y	7314.62	7235.57	−79.05
(018)	68.77° Y	7305.47	7210.04	−95.43
$(01\underline{14})$	77.48° Y	7315.95	7212.93	−103.02
(006)	Z	7328.20	7221.55	−106.65
$(10\underline{10})$	107.27° Y	7298.94	7200.01	−98.93
(104)	127.85° Y	7158.99	7091.47	−67.52
(306)	147.24° Y	6855.49	6825.97	−29.52
(202)	162.17° Y	6656.29	6650.59	−5.70
(110)	X	6544.53	6547.31	+2.78
(223)	15.57° X	6714.03	6706.52	−7.51
(113)	29.13° X	6970.74	6944.45	−26.29
(229)	39.89° X	7128.89	7083.44	−45.45
(116)	48.10° X	7206.55	7145.59	−60.96
$(11\underline{12})$	65.84° X	7286.28	7194.37	−91.91
(410)	100.89° X(Z)	6738.03	6740.99	+2.96

pendence on SAW velocities were used. By considering the dependence of each constant on SAW velocity and selecting appropriate specimens and propagation directions, the acoustical physical constants can be determined with higher accuracy using SAW velocities.

VII. Conclusion

In this paper, we determined all of the independent components of acoustical physical constants of commercially available, SAW-grade $LiNbO_3$ and $LiTaO_3$ single crystals by measuring the bulk acoustic wave velocities, dielectric constants, and densities of many plate specimens. Furthermore, we examined the maximum error that may occur in each constant by considering the dependence of each constant on the measured velocities. We then com-

TABLE X
COMPARISON OF LONGITUDINAL WAVE VELOCITIES MEASURED FOR $LiTaO_3$ SPECIMENS WITH THOSE CALCULATED USING KOVACS' CONSTANTS.

Specimen		Measured (m/s)	Calculated (m/s)	Difference (m/s)
(300)	Y	5746.11	5753.07	+6.96
(042)	9.21° Y	5965.66	5972.45	+6.79
(012)	32.98° Y	6332.93	6327.96	−4.97
$(02\underline{10})$	58.35° Y	6289.55	6277.44	−12.11
(018)	68.93° Y	6226.76	6216.90	−9.86
(006)	Z	6174.94	6168.97	−5.97
$(10\underline{10})$	107.13° Y	6174.73	6167.17	−7.56
(104)	127.62° Y	6058.13	6051.42	−6.71
(306)	147.02° Y	5752.84	5751.02	−1.82
(202)	162.03° Y	5543.54	5545.27	+1.73
(110)	X	5589.17	5588.52	−0.65
(113)	29.33° X	5995.42	5991.10	−4.32
(116)	48.34° X	6179.72	6169.47	−10.25
(119)	59.32° X	6204.09	6193.21	−10.88
$(11\underline{12})$	66.02° X	6201.17	6191.22	−9.95
(410)	100.89° X(Z)	5705.21	5710.06	+4.85

pared the measured longitudinal velocities that were not used to determinine the constants with the calculated values using the constants determined here and found a difference of 1 m/s or less. From this result, we can say that the acoustical physical constants determined here can yield bulk acoustic wave velocities with an accuracy of four significant digits.

Acknowlegments

The authors are grateful to T. Sasamata of Yamaju Ceramics Co., Ltd. for growing the crystals and to Y. Okada of Kogakugiken Co., Ltd. for preparing the specimens. We also express our thanks to N. Akashi, J. Hirohashi, and S. Nishiyama for cooperation during experiments.

References

[1] A. W. Warner, M. Onoe, and G. A. Coquin, "Determination of elastic and piezoelectric constants for crystals in class (3m)," *J. Acoust. Soc. Amer.*, vol. 42, pp. 1223–1231, Dec. 1967.

[2] T. Yamada, N. Niizeki, and H. Toyoda, "Piezoelectric and elastic properties of lithium niobate single crystals," *Jpn. J. Appl. Phys.*, vol. 6, pp. 151–155, Feb. 1967.

[3] T. Yamada, H. Iwasaki, and N. Niizeki, "Piezoelectric and elastic properties of $LiTaO_3$: temperature characteristics," *Jpn. J. Appl. Phys.*, vol. 8, pp. 1127–1132, Sep. 1969.

[4] R. T. Smith and F. S. Welsh, "Temperature dependence of the elastic, piezoelectric, and dielectric constants of lithium tantalate and lithium niobate," *J. Appl. Phys.*, vol. 42, pp. 2219–2230, May 1971.

[5] V. V. Chkalova, V. S. Bondarenko, G. O. Fokina, and F. N. Strizhevskaya, "Temperature dependences of the dielectric, piezoelectric, and elastic properties of lithium niobate single crystals," *Bull. Acad. Sci. USSR*, vol. 35, pp. 1712–1715, 1971.

[6] A. P. Korolyuk, L. Ya. Matsakov, and V. V. Vasil'chenko, "Determination of elastic and piezoelectric constants of lithium niobate single crystals," *Soviet Phys. - Crystallography*, vol. 15, pp. 893–896, Mar.-Apr. 1971.

[7] Y. Nakagawa, K. Yamanouchi, and K. Shibayama, "Third-order elastic constants of lithium niobate," *J. Appl. Phys.*, vol. 44, pp. 3969–3974, Sep. 1973.

[8] R. A. Graham, "Second- and third-order piezoelectric stress constants of lithium niobate as determined by the impact-loading technique," *J. Appl. Phys.*, vol. 48, pp. 2153–2163, Jun. 1977.
[9] I. A. Dan'kov, E. F. Tokarev, G. S. Kudryashov, and K. G. Belobaev, "Elastic, piezoelectric, and dielectric properties of monocrystalline lithium niobate between 78 and 800°K," *Inorg. Mat.*, vol. 19, pp. 1049–1054, Jul. 1983.
[10] G. Kovacs, M. Anhorn, H. E. Engan, G. Visintini, and C.C.W. Ruppel, "Improved material constants for $LiNbO_3$ and $LiTaO_3$," in *Proc. 1990 IEEE Ultrason. Symp.*, Honolulu, Hawaii, Dec. 1990, pp. 435–438.
[11] R. V. Damle, "Elastic constants of lithium niobate," *J. Phys. D: Appl. Phys.*, vol. 25, pp. 1091–1095, Jul. 1992.
[12] K. Taki and Y. Shimizu, "Material constants of $LiTaO_3$ determined from surface acoustic wave velocities," *Jpn. J. Appl. Phys.*, vol. 33, pp. 2976–2978, May 1994.
[13] I. Takanaga, J. Hirohashi, and J. Kushibiki, "Homogeneity evaluation of $LiNbO_3$ and $LiTaO_3$ single crystals for determining acoustical physical constants," *Jpn. J. Appl. Phys.*, vol. 38, pp. 3201–3203, May 1999.
[14] J. Kushibiki, N. Akashi, T. Sannomiya, N. Chubachi, and F. Dunn, "VHF/UHF range bioultrasonic spectroscopy system and method," *IEEE Trans. Ultrason., Ferroelect., Freq. Contr.*, vol. 42, pp. 1028–1039, Nov. 1995.
[15] J. Kushibiki and I. Takanaga, "Elastic properties of single- and multi-domain crystals of $LiTaO_3$," *J. Appl. Phys.*, vol. 81, pp. 6906–6910, May 1997.
[16] *IEEE Standard on Piezoelectricity*, Standard 176, 1987.
[17] H. A. Bowman and R. M. Schoonover, "Procedure for high precision density determinations by hydrostatic weighing," *J. Res. Nat. Bur. Stand.*, vol. 71C, pp. 179–198, Jul.-Aug. 1967.
[18] J. G. Gualtieri, J. A. Kosinski, and A. Ballato, "Piezoelectric materials for acoustic wave applications," *IEEE Trans. Ultrason., Ferroelect., Freq. Contr.*, vol. 41, pp. 53–59, Jan. 1994.

Jun-ichi Kushibiki (M'83) was born in Hirosaki, Japan, on November 23, 1947. He received the B.S., M.S., and Ph.D. degrees in electrical engineering from Tohoku University, Sendai, Japan, in 1971, 1973, and 1976, respectively.

In 1976, he became a research associate at the Research Institute of Electrical Communication, Tohoku University. In 1979, he joined the Department of Electrical Engineering, Faculty of Engineering, Tohoku University, where he was an associate professor from 1988 to 1993 and became a professor in 1994. He has been studying ultrasonic metrology, especially acoustic microscopy and its applications, and has established a method of material characterization by line-focus-beam acoustic microscopy. He also has been interested in biological tissue characterization in the higher frequency range applying both bulk and acoustic microscopy techniques.

Dr. Kushibiki is a member of the Acoustical Society of America; the Institute of Electronics, Information, and Communication Engineers of Japan; the Institute of Electrical Engineers of Japan; the Acoustical Society of Japan; and the Japan Society of Ultrasonics in Medicine.

Izumi Takanaga was born in Toyama Prefecture, Japan, on February 3, 1973. She received the B.S. and M.S. degrees in electrical engineering from Tohoku University, Sendai, Japan, in 1995 and 1997, respectively.

She is currently studying toward the Ph.D. degree at Tohoku University. Her research interests include accurate measurement of the elastic properties of piezoelectric materials and investigation of the domain structures of ferroelectric materials.

Miss Takanaga is a member of the Acoustical Society of Japan.

Mototaka Arakawa was born in Sendai, Japan, on January 19, 1971. He received the B.S. and M.S. degrees in electrical engineering from Tohoku University, Sendai, Japan, in 1993 and 1995, respectively.

He is currently studying toward the Ph.D. degree at Tohoku University. His research interests include developments of the measurement methods of elastic constants of solid materials and of the calibration method of the line-focus-beam acoustic microscopy system.

Mr. Arakawa is a member of the Acoustical Society of Japan and the Institute of Electronics, Information, and Communication Engineers of Japan.

Toshio Sannomiya was born in Miyagi Prefecture, Japan, on October 3, 1938. He graduated from the Sendai Radio High School in 1959.

From 1959 to 1978, he was with the Research Institute of Electrical Communication, Tohoku University, Sendai, Japan. Since 1979, he has been at the Department of Electrical Engineering, Faculty of Engineering, Tohoku University. He received the Ph.D. degree in electrical engineering from Tohoku University in 1996. Since 1998, he has been a research associate at the Department of Electrical Engineering, Graduate School of Engineering, Tohoku University. He has engaged in studies of ultrasonic transducers, ultrasonic measurements, and acoustic microscopy.

Dr. Sannomiya is a member of the Acoustical Society of Japan and the Japan Society of Ultrasonics in Medicine.